Sensors & Transducers, Vol. 228, Issue 12, December 2018, pp. 71-78

www.sensorsportal.com

Sensors & Transducers

Published by IFSA Publishing, S. L., 2018
http://www.sensorsportal.com

Geometry Dependence of the Response of Inter-digital Capacitive Structures: A Finite Element Analysis

[1] Sheeja P. George, [2] Johney Issac and [3] Jacob Philip

[1] College of Engineering, Chengannur, Alappuzha, 689121, Kerala, India
[2] Department of Instrumentation, Cochin University of Science and Technology, Cochin, 682022, Kerala, India
[3] Amal Jyothi College of Engineering, Kanjirappally, Kottayam 686518, Kerala, India
[1] Tel.: +91-949-595-6861
[1] E-mail: sheejapgmanoj@yahoo.com

Received: 19 July 2018 /Accepted: 30 November 2018 /Published: 31 December 2018

Abstract: Inter-digital capacitive sensors with planar geometry are under development for a variety of applications. Variations in the geometry of such planar inter-digital capacitive transducer structures exhibit changes in their response in terms of the corresponding capacitance variations. In this work we present a performance evaluation of the response of inter-digital capacitive structures based on the differences in the geometry of their inter-penetrating comb patterns. All the geometries under consideration are fabricated following the same procedure on printed circuit boards made of FR4. The capacitance values for each configuration have been measured directly. The capacitance values for the same configurations have been evaluated by simulation using the Finite element analysis tool, ANSYS. Parameters like finger spacing, relative permittivity and medium thickness have been varied in simulation and system performance analyzed. A comparison between measured and simulated values have been carried out and the results are presented. The results enable one to predict the capacitance values and sensor performance of IDC structures of this type. The procedure can be adapted to other types of structures as well.

Keywords: Inter-digital capacitive structures, Inter-digital transducers, Inter-penetrating comb patterns, Finite element analysis.

1. Introduction

Co-planar periodic finger-like patterns of parallel inter-penetrating electrodes form inter-digital capacitive (IDC) structures, and their effective capacitances increase as the effective area increases. The fringing electric field lines generated between the electrodes make it a versatile device in applications like nondestructive testing, MEMS, microwave filters, and as sensors to measure parameters such as acoustic wave intensity, pressure, humidity, proximity, level [1-8] etc. They also find applications such as biosensors and in food testing [9-11]. A review article discussing the various aspects of inter-digital sensors and transducers can be found in literature [12]. The design and use of inter-digital electrodes began as early as in 1891, found in the patent of Tesla [13]. The very common features that attract device designers to inter-digital structures are the one sided access control of the signal strength, imaging capability, simplified modeling and wide frequency spectrum [12].

Typical co-planar inter-digital structures formed from parallel plate capacitors, along with the corresponding fringing field directions, are depicted in Fig. 1.

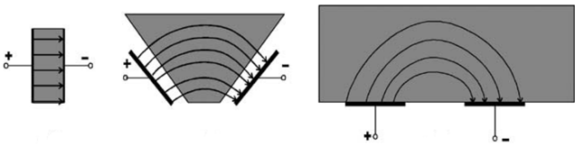

Fig. 1. Typical co-planar structures formed from Parallel plate capacitors [12].

The capacitance between the positive and negative electrode terminals of a capacitor is

$$C = \frac{\varepsilon_0 \, \varepsilon_r \, A}{d}, \tag{1}$$

where C is the capacitance, ε_0 is the permittivity of free space, ε_r is the relative permittivity of the medium, A is the area of cross-section and d is the separation between the electrodes. Inter-digital capacitor has the advantage of providing more capacitance per unit chip area than a two-plate parallel configuration [14]. The most important parameters for any sensor, the sensitivity and selectivity, have a strong link with sensor geometry. The effect of electrode geometry on the performance of such Inter-digital transducers (IDTs) has appeared in literature. The capacitance varies depending on the material dielectric constant as well as the electrode geometry [15-18]. The dependence of the electrode thickness, length and the number of electrode fingers on the change of capacitance is investigated in this work. A modified sensor design used for food inspection can be found in literature [19]. A model configuration of an inter-digital capacitive structure is illustrated in Fig. 2 [20].

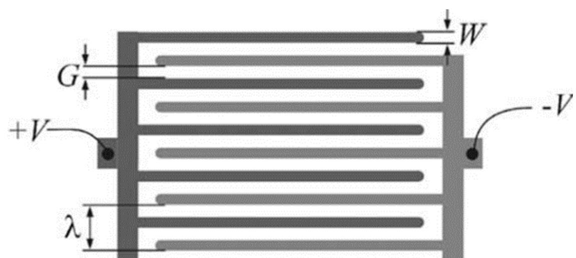

Fig. 2. Inter-digital capacitive structure under investigation [20].

In Fig. 2 each finger is of width W and G is the gap between the fingers. λ =2(W+G) is the spatial wavelength and L is the length of the fingers. Each comb group is connected either to the positive or negative terminal of the potential source.

One of the key features of an inter-digital capacitive structure is the simplicity of modeling with numerical tools [21]. Network model approach as well as CAD based modeling have been carried out and reported on them [22-24]. The Finite element analysis helps to handle complex geometries and is used extensively for sensor modeling, optimization, and performance evaluation, especially for structures that are difficult to model analytically or otherwise. All the modeling work reported for inter-digital structures so far considered only a particular geometry for a specific application. A comparative study of the performance of inter-digital structures according to the number of fingers, finger widths and gaps between fingers has been carried out and illustrated in this work. We present results of the analysis of various inter-digital capacitive structures by simulation using the Finite element analysis tool ANSYS and compare the computed capacitance values obtained with those from direct measurements.

2. Configuration of IDC Structures and Measurements

The basic comb structure considered in this work is with W=381µm, G=889µm and L=8890µm (see Fig. 2). Geometrical difference between structures is introduced by changing the values of W and L. Changes introduced in to periodic pattern correspondingly changes the capacitance values. The number of finger pairs is varied from four to six, which enhances the total number of fingers from eight to twelve with equal number of positive and negative terminals, as shown in Fig. 3.

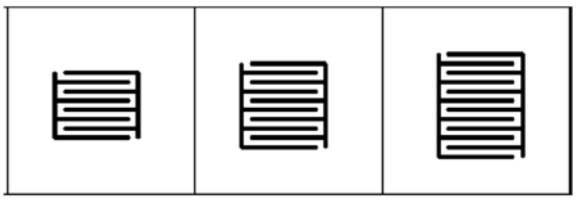

Fig. 3. Configurations of IDC structures with finger pairs of four to six.

Then the structural variations are introduced by fixing the total number of fingers and then making a distinction in the number of positive and negative electrodes. Accordingly, we present inter-digital capacitors with total number of fingers at 13 [1_2_1, 1_3_1, 1_5_1 and 1_11_1], 15 [1_6_1 and 1_13_1], 16 [1_2_1, 1_4_1 and 1_14_1] and 17 [1_3_1, 1_7_1 and 1_15_1], as demonstrated in Figs. 4, 5, 6 and 7. Table 1 provides the terminal distribution for different configurations shown in the Figs. 4, 5, 6 and 7.

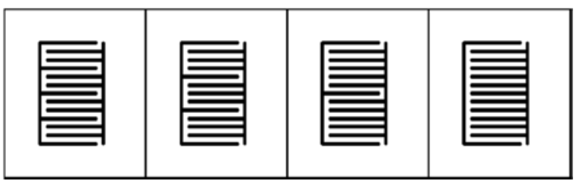

Fig. 4. Configurations of IDC structures with 13 fingers [1_2_1, 1_3_1, 1_5_1 & 1_11_1].

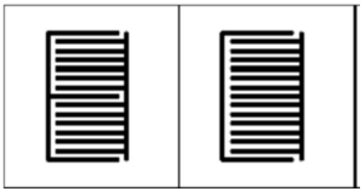

Fig. 5. Configurations of IDC structures with 15 fingers [1_6_1 & 1_13_1].

Fig. 6. Configurations of IDC structures with 16 fingers [1_2_1, 1_4_1 & 1_14_1].

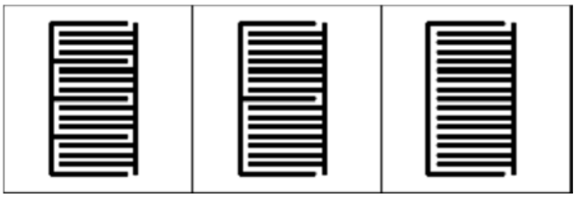

Fig. 7. Configurations of IDC structures with 17 fingers [1_3_1, 1_7_1 & 1_15_1].

Table 1. Terminal distributions for different IDC configurations, shown in Figs. 4 to 7.

No. of fingers	Configuration	No. of positive terminals	No. of negative terminals
13	1_2_1	5	8
	1_3_1	4	9
	1_5_1	3	10
	1_11_1	2	11
15	1_6_1	3	12
	1_13_1	2	13
16	1_2_1	6	10
	1_4_1	4	12
	1_14_1	2	14
17	1_3_1	5	12
	1_7_1	3	14
	1_15_1	2	15

In each case the width of the fingers (W) and their length (L) are altered to evaluate the dependence of each on the resultant capacitance. The finger width is altered with values as 381 μm, 508 μm, 635 μm and 762 μm. The lengths of the fingers are changed to values of 8890 μm, 7620 μm and 6350 μm. This structural variation is executed in all the geometries. Fabrication was carried out for all the variations.

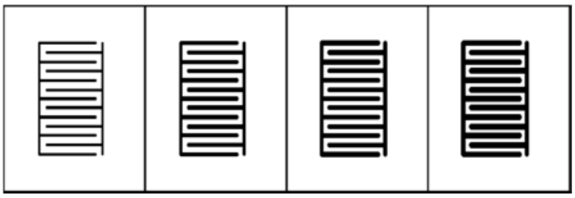

Fig. 8. Finger width (W), variation of 381 μm, 508μm, 635 μm and 762 μm in the case of six pair IDC.

Fig. 9. Length of the finger (L), variation of m in the case of 6 pair IDC.

All the inter-digital capacitors are planar in their geometrical structure and are comparatively simple to fabricate using the usual PCB fabrication techniques. The comb structure is designed using Proteus and is printed onto a tracing sheet. Screen printing method has been used for the fabrication of the structures. The design on the tracing sheet is transferred to five-star film by UV exposure and then on to FR4 board. The unwanted portions in the board are removed by etching and traces of the inter-digital structures remain affixed on to the board. Inter-digital structures with varying finger widths (W) and finger lengths (L), as depicted in Figs. 3 to 7, have been fabricated.

Direct measurement of the effective capacitance of each of the structures has been carried out using the LCR measurement feature of an Impedance Analyzer (Make: Hioki, Model: IM 3570). The instrument allows test signal of DC or a band of frequency in the range 4 Hz to 5 MHz with output levels varying from 5 mV to 5 V. The four-terminal probe used during measurements provides improved accuracy.

3. Simulation of IDC Structures

Finite Element Analysis (FEA) is a tool of numerical method for solving engineering problems and commercial packages are available for the same. In this work we have made use of the FEA tool ANSYS 15.0, because it enables to perform the desired electrostatic field analysis effectively. With electrostatic field analysis using FEA, electric field distribution and electric scalar potential due to charge distribution or applied potential can be determined. The load we apply as input in this analysis is the voltage. The elements that are used in the charge based electrostatic analysis are PLANE 121, SOLID 122 and SOLID 123. In the present analysis we consider PLANE 121 which is a 2D element of 8 nodes with the degree of freedom for voltage at each node. For 3D analysis SOLID 122, a charge based 20 node element with degree of freedom for voltage, is used.

The electrostatic analysis begins with building the model by selecting the appropriate element which is made available with setting the preference to electric field. The element type and the material property (permittivity) are to be defined before the required geometry is generated. The bottom up approach is taken to build the model where it starts with creating key points and then lines, areas and volumes are defined as the case may be. By meshing the model nodes and elements are created. Meshing controls enables to establish the desired mesh density. The features like coupled degrees of freedom and constraint equation can be added to the nodes and elements as required. The loads for electrostatic analysis can be applied on the solid model or on the finite element model. The solution is obtained through the SOLVE command and the general post processor menu provides a review of the results of the analysis. The model built in ANSYS and the meshed structure is given in Fig. 10 and Fig. 11 for six pair IDC. The same procedure is followed for all the geometric structure.

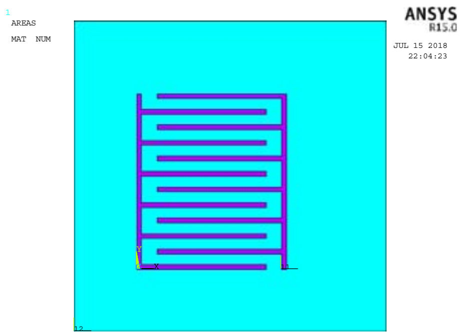

Fig. 10. IDC modeling in ANSYS for six pair structure.

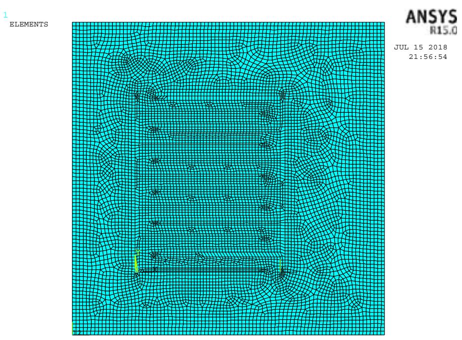

Fig. 11. Meshed IDC structure (six pair).

The capacitance calculation for an electrostatic system is based on the energy principle and is computed using the CMATRIX Macro [25]. Knowledge of the capacitance is essential for the design of electrostatic devices, MEMS etc. One has to define the electrodes in the geometry appropriately and CMATRIX calculates the capacitance from the stored energy across the electrodes.

4. Results and Discussion

Measurement values of effective capacitance have been obtained directly from the LCR meter, and the corresponding simulation values using FEA tool ANSYS as outlined above. Measurement and simulation are done on all the fabricated inter-digital structures. Variations in capacitance values with variations in different structural parameters are outlined below. For the graphical representation the notation “meas” denotes the measured value and “sim” denotes the simulated value. In all figures results from simulation and measurement are shown separately for each configuration.

4.1. Change in Finger Width (W)

First, variations in the structure have been incorporated by changing the width (W) of the fingures. Finger widths chosen for experimentation are 381 µm, 508 µm, 635 µm and 762 µm, keeping the finger length costant. As the finger width increases the effective area increases and the capacitance increases. The results are shown in Figs. 12 to 16.

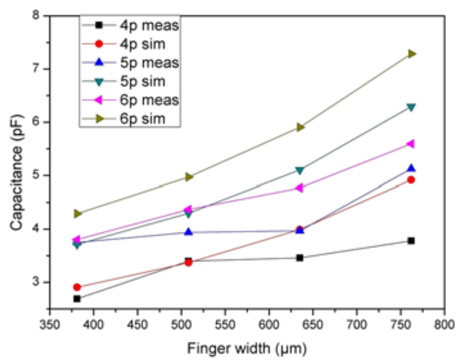

Fig. 12. Capacitance values obtained from measurement and simulation for four to six pairs.

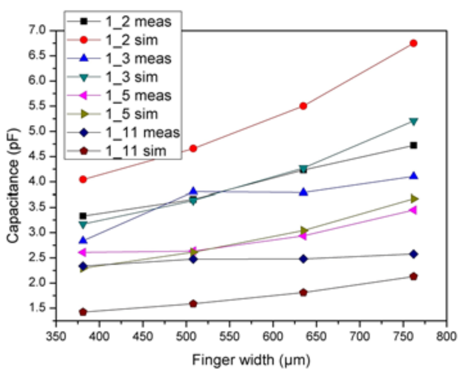

Fig. 13. Capacitance values obtained from measurement and simulation for 13 fingers.

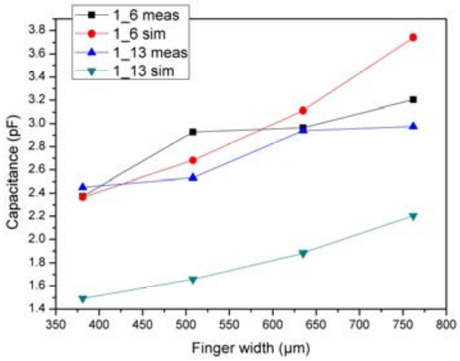

Fig. 14. Capacitance values obtained from measurement and simulation for 15 fingers.

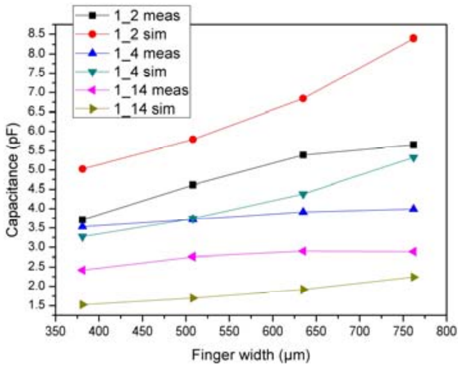

Fig. 15. Capacitance values obtained from measurement and simulation for 16 fingers.

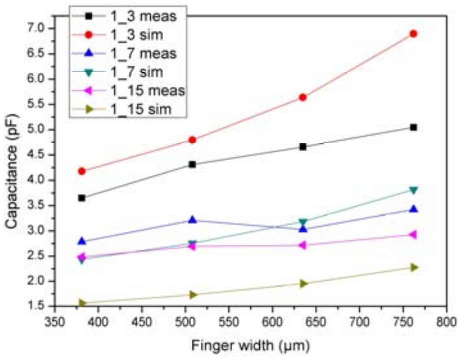

Fig. 16. Capacitance values obtained from measurement and simulation for 17 fingers.

4.2. Change in Length of the Fingers (L)

We have fabricated inter-digital capacitive structures with length of fingers at 6350 μm, 7620 μm and 8890 μm, with width of the finger and the gap between them kept constant. As the length of the finger is increased the distance between the electrodes decreases and correspondingly the capacitance value increases. The results of measurement and simulation are shown in Figs. 17 to 21. It can be noted that, in general, the capacitance value increases with length of the fingers for an IDC comb structure.

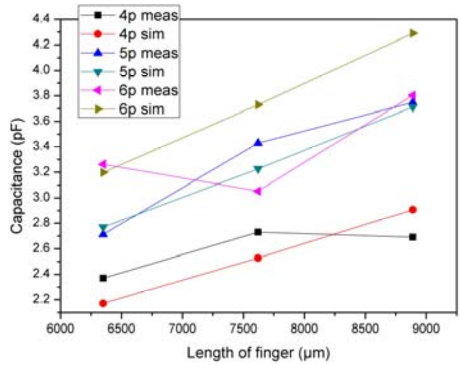

Fig. 17. Capacitance variation with the change in length (L) of the fingers for four to six pairs.

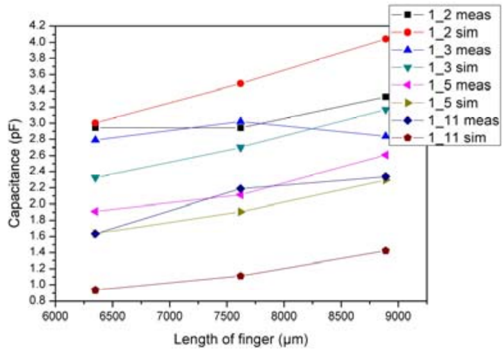

Fig. 18. Capacitance variation with the change in length (L) of the fingers for 13 fingers.

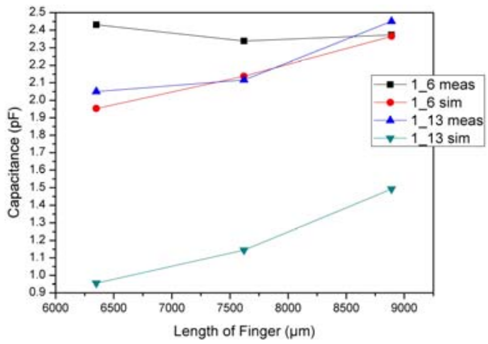

Fig. 19. Capacitance variation with the change in length (L) of the fingers for 15 fingers.

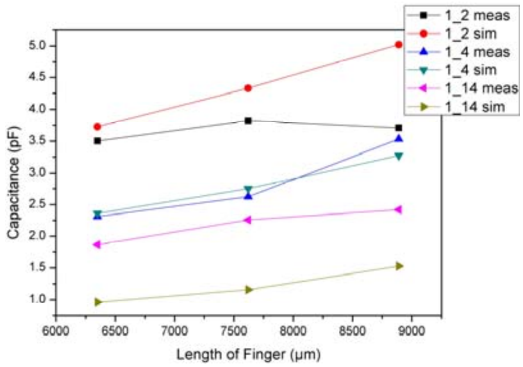

Fig. 20. Capacitance variation with the change in length (L) of the fingers for 16 fingers.

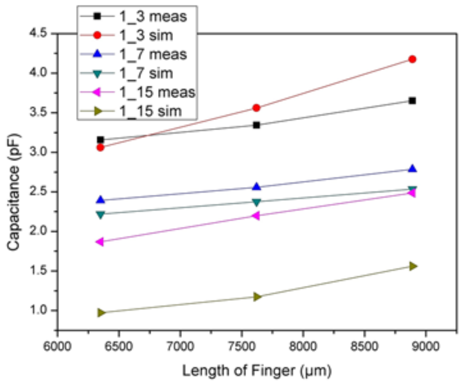

Fig. 21. Capacitance variation with the change in length (L) of the fingers for 17 fingers.

In order to carry out further analysis of inter-digital structures with change in gap between fingers, substrate thickness and dielectric medium, we have selected the configuration having close agreement between the measured and simulated values. Accordingly, the structures designated as 1_5_1 (13), 1_6_1 (15), 1_4_1 (16) and 1_7_1 (17) have been selected for further analysis. It can be noted from Figs. 12 to 21 that the agreement between measured and simulated capacitance values are the best for these selected structures. For equal number of positive and negative terminals capacitance value increases as the number of fingers increases. It is comparable to the case of parallel plate capacitor where the area is directly proportional to the capacitance.

Though the numerical values of the measured capacitance and the corresponding values obtained from simulation are not is very good agreement always, it can be noted that their variations due to changes in geometrical parameters, in general, are in agreement. The differences in numerical values in many cases may be due to uncertainties in the measurement of capacitance and limitations of the finite element analysis adopted in the work. For the changes in gap between fingers, dielectric medium changes and medium thickness the result obtained are through simulation only.

4.3. Change in Gap Between Fingers (G)

The gap between the fingers has been varied keeping the width of the finger and its length constant. The results are shown in Fig. 22. It can be noted that the capacitance values, in general, decreases exponentially with increase in gap between fingers for comb type IDC structures.

4.4. Change of Top Layer Material

Material identification is one of the prime applications of sensors. IDC structures have a major role as they have the ability to vary the capacitance depending on the dielectric constant of the material located on top of the plates. The capacitance change is given by C = εrC0, where εr is the relative permittivity of the material under consideration and C0 is the capacitance without the dielectric.

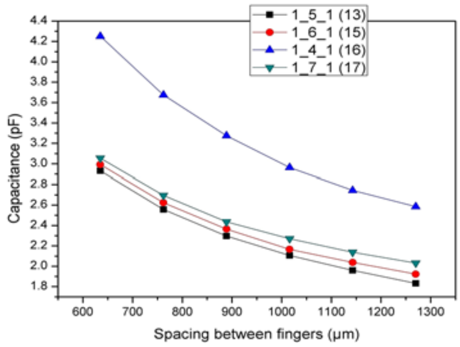

Fig. 22. Variation in capacitance with change in gap between the fingers.

For the simulation IDC structure with the basic physical dimension is considered and the top layer is formed using SOLID element for which the dielectric constant can be varied. It can be observed that the capacitance increases with the increase in the dielectric constant of the top layer material. The result is as shown in Fig. 23.

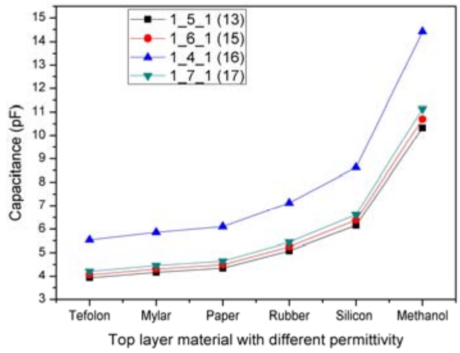

Fig. 23. Capacitance variation with respect to change in top layer material.

4.5. Change in Top Layer Thickness

Keeping the parameters G, W and L constant the dielectric medium thickness is varied. Capacitance change is prominent as the thickness variation is initiated and the percentage variation decreases as thickness increases. The result is as shown in Fig. 24.

5. Conclusions

The results presented in this paper show that for planar IDC structures one can arrive at capacitance values and their variations with geometry of the structures by carrying out modeling and finite element analysis of the structures. There is good agreement between results from analysis and physical measurements. The results show that it is possible to predict sensor parameters and performance for any comb-type structure with variations in geometry. Moreover, without any loss of generality, the procedure followed in this work can be adapted to IDC structure configurations of any kind to predict their performance for any application.

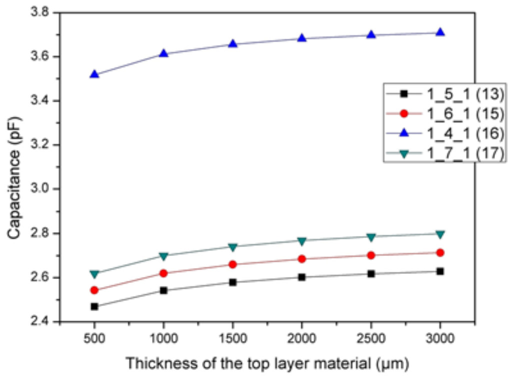

Fig. 24. Capacitance variation with respect to change in top layer thickness.

References

[1]. J. Jin, S. T. Quek, Q. Wang, Design of Interdigital transducers for crack detection in plates, *Ultrasonics*, Vol. 43, Issue 6, 2005, pp. 481-493.

[2]. A. H. M. Habib Ahsan, C. F. Lange, W. Moussa, Development of a Humidity Microsensor with Thermal Reset, in *Proceedings of the IEEE International Conference on MEMS, NANO and Smart Systems,* 2003.

[3]. K. A. Jose, W. D. Suh, P. B. Xavier, V. K. Varadan, V. V. Varadan, Surface acoustic wave MEMS gyroscope, *Wave Motion*, Vol. 36, 2002, pp. 367–381.

[4]. Li Zhu, Vijay Devabhaktuni, Chunyan Wang, Ming Yu, Adjustable Bandwidth Filter Design Based on Interdigital Capacitors, *IEEE Microwave and Wireless Components Letters*, Vol. 18, Issue 1, 2008.

[5]. M. J. Vellekoop, Acoustic wave sensors and their technology, *Ultrasonics*, Vol. 36, 1998, pp. 7-14.

[6]. R. M. White, Acoustic Sensors for Physical, Chemical and Biochemical Applications, in *Proceedings of the IEEE International Frequency Control Symposium,* 1998.

[7]. Xuesong Ye, Lu Fang, Bo Liang, Qiong Wang, Xuejun Wang, Lisong He, Weibin Bei, Wen H. Ko, Studies of a high-sensitive surface acoustic wave sensor for passive wireless blood pressure measurement, *Sensors and Actuators A,* Vol. 169, Issue 1, 2011, pp. 74-82.

[8]. K. Chetpattananondh, T. Tapoanoi, P. Phukpattaranont, N. Jindapetch, A self-calibration water level measurement using an interdigital capacitive sensor, *Sensors and Actuators A,* Vol. 209, 2014, pp. 175-182.

[9]. Yang Choon Lim, Abbas Kouzani, Akif Kaynak, Riyadh Al-Ameri, Wei Duan, A Micromechanical Biosensor with Interdigitated Capacitor Readout, in *Proceedings of the IEEE International Conference on Complex Medical Engineering,* 2011.

[10]. S. C. Mukhopadhyay, C. P. Gooneratne, G. S. Gupta, S. N. Demidenko, A Low-Cost Sensing System for Quality Monitoring of Dairy Products, *IEEE Transactions on Instrumentation and Measurement,* Vol. 55, Issue 4, 2006, pp. 1331-1338.

[11]. Subhas Chandra Mukhopadhyay, Chnithaka P. Gooneratne, A Novel Planar-Type Biosensor for Noninvasive Meat Inspection, *IEEE Sensors Journal*, Vol. 7, Issue 9, 2007, pp. 1340-1346.

[12]. A. V. Mamishev, K. Sundara-Rajan, Fumin Yang, Yanqing Du, M. Zahn, Interdigital sensors and transducers, in *Proceedings of the IEEE*, Vol. 92, Issue 5, 2004, pp. 808-845.

[13]. Tesla N., Electric condenser, *U.S. Patent 1891*, No. 464, 667.

[14]. Scott A. Miller, Kimberly L. Turner, Noel C. MacDonald, Microelectromechanical scanning probe instruments for array architectures, *Review of Scientific Instruments*, Vol. 68, Issue 11, 1997, pp. 4155-4162.

[15]. Igreja R., Dias C. J., Dielectric response of interdigital chemo-capacitors: The role of the sensitive layer thickness, *Sensors and Actuators B,* Vol. 115, Issue 1, 2006, pp. 69-78.

[16]. Mamishev A. V., Takahashi A. R., Du Y., Lesieutre B. C., M. Zahn, Assessment of performance of fringing electric field sensor arrays, in *Proceedings of the IEEE Conf. Electrical Insulation and Dielectric Phenomena,* 2002, pp. 918-921.

[17]. Li X. B, Larson S. D., Zyuzin A. S., Mamishev A. V., Design Principles for Multichannel Fringing Electric Field Sensors, *IEEE Sensors Journal*, 2006, Vol. 6, Issue 2, pp. 434-440.

[18]. Lakin K. M., Mih D. W. T., Tarr R. M., A New Interdigital Electrode Transducer Geometry, *IEEE Transactions on Microwave Theory and Techniques*, Vol. MTT-22, Issue 8, 1974, pp. 763-768.

[19]. Mukhopadhyay S. C., Novel Planar Electromagnetic Sensors: Modeling and Performance Evaluation, *Sensors*, Vol. 5, Issue 12, 2005, pp. 546-579.

[20]. Igreja Rui, Dias C. J., Analytical evaluation of the interdigital electrodes capacitance for a multi-layered structure, *Sensors and Actuators A,* Vol. 112, 2004, pp. 291-301.

[21]. Mahapatra D. R., Singhal A, Gopalakrishnan S., Numerical Analysis of Lamb Wave Generation in Piezoelectric Composite IDT, *IEEE Transactions on Ultrasonics, Ferroelectrics, and Frequency Control,* Vol. 52, Issue 10, 2005, pp. 1851-1860.

[22]. M. P. de Cunha, E. L. Adler, A Network Model for Arbitrarily Oriented IDT Structures. *IEEE Transactions on Ultrasonics, Ferroelectrics, and Frequency Control,* Vol. 40, Issue 6, 1993, pp. 622-629.

[23]. Nihad Dib, Qiu Zhang, Ulrich Rohde, New CAD model of the microstrip Interdigital Capacitor, *Active and Passive Electronic Components,* Vol. 27, Issue 4, 2004, pp. 237-245.

[24]. Nihad Dib, Jehad Ababneh, Amjad Omar, CAD Modeling of Coplanar Waveguide Interdigital Capacitor, *Wiley Inter Science*, 2005, pp. 551-559.

[25]. ANSYS Mechanical APDL Theory Reference Release 15.0, *ANSYS, Inc,* 2013.

Published by International Frequency Sensor Association (IFSA) Publishing, S. L., 2018 (http://www.sensorsportal.com).